

Article

Amaryllidaceae-Type Alkaloids from *Pancreatium maritimum*: Apoptosis-Inducing Effect and Cell Cycle Arrest on Triple-Negative Breast Cancer Cells

Shirley A. R. Sancha ¹, Adriana V. Gomes ², Joana B. Loureiro ², Lucília Saraiva ^{2,*}
and Maria José U. Ferreira ^{1,*}

¹ Faculty of Pharmacy, Research Institute for Medicines (iMed.Ulisboa), Universidade de Lisboa, Av. Prof. Gama Pinto, 1649-003 Lisbon, Portugal

² LAQV/REQUIMTE, Laboratório de Microbiologia, Departamento de Ciências Biológicas, Faculdade de Farmácia, Universidade do Porto, 4050-313 Porto, Portugal

* Correspondence: lucilia.saraiva@ff.up.pt (L.S.); mjuferrera@ff.ulisboa.pt (M.J.U.F.); Tel.: +351-217946475 (M.J.U.F.); Fax: +351-217946470 (M.J.U.F.)

Abstract: Aiming to find Amaryllidaceae alkaloids against breast cancer, including the highly aggressive triple-negative breast cancer, the phytochemical study of *Pancreatium maritimum* was carried out. Several Amaryllidaceae-type alkaloids, bearing scaffolds of the haemanthamine-, homolycorine-, lycorine-, galanthamine-, and tazettine-type were isolated (3–11), along with one alkamide (2) and a phenolic compound (1). The antiproliferative effect of compounds (1–11) was evaluated by the sulforhodamine B assay against triple-negative breast cancer cell lines MDA-MB-231 and MDA-MB-468, breast cancer cells MCF-7, and the non-malignant fibroblast (HFF-1) and breast (MCF12A) cell lines. The alkaloids 3, 5, 7, and 11 showed significant growth inhibitory effects against all breast cancer cell lines, with IC₅₀ (half-maximal inhibitory concentration) values ranging from 0.73 to 16.3 μM. The homolycorine-type alkaloid 7 was selected for further investigation in MDA-MB-231 cells. In the annexin-V assay, compound 7 increased cell death by apoptosis, which was substantiated, in western blot analyses, by the increased expression of the pro-apoptotic protein Bax, and the decreased expression of the anti-apoptotic protein Bcl-xL. Consistently, it further stimulated mitochondrial reactive oxygen species (ROS) generation. The antiproliferative effect of compound 7 was also associated with G2/M cell cycle arrest, which was supported by an increase in the p21 protein expression levels. In MDA-MB-231 cells, compound 7 also exhibited synergistic effects with conventional chemotherapeutic drugs such as etoposide.

Keywords: amaryllidaceae alkaloids; *Pancreatium maritimum*; triple-negative breast cancer; antiproliferative effect; apoptosis; cell cycle



Citation: Sancha, S.A.R.; Gomes, A.V.; Loureiro, J.B.; Saraiva, L.; Ferreira, M.J.U. Amaryllidaceae-Type Alkaloids from *Pancreatium maritimum*: Apoptosis-Inducing Effect and Cell Cycle Arrest on Triple-Negative Breast Cancer Cells. *Molecules* **2022**, *27*, 5759. <https://doi.org/10.3390/molecules27185759>

Academic Editors: Vassya Bankova and Milena Popova

Received: 27 July 2022

Accepted: 2 September 2022

Published: 6 September 2022

Publisher's Note: MDPI stays neutral with regard to jurisdictional claims in published maps and institutional affiliations.



Copyright: © 2022 by the authors. Licensee MDPI, Basel, Switzerland. This article is an open access article distributed under the terms and conditions of the Creative Commons Attribution (CC BY) license (<https://creativecommons.org/licenses/by/4.0/>).

1. Introduction

Cancer is a major health concern worldwide, mainly attributed to drug resistance. Breast cancer is the most frequent cancer diagnosed among women [1]. Triple-negative breast cancer, which is well known for its therapeutic resistance, is an aggressive subtype of breast cancer with defective expression of estrogen and progesterone receptors and a lack of human epidermal growth factor receptor 2. Triple-negative breast cancer is generally associated with hereditary conditions, representing 10–15% of the newly diagnosed breast cancer [2,3]. The treatment of this type of breast cancer is mainly based on standard chemotherapy, including platinum drugs, and more recently on poly (ADP-ribose) polymerase (PARP) inhibitors. However, the use of these anticancer drugs has been limited by the occurrence of drug resistance, related to the complexity of the tumor microenvironment and heterogeneity, which is characterized by the interaction of multiple factors and signaling pathways [4,5]. Despite all efforts that have been developed in the discovery of new

chemotherapeutic agents, targeting triple-negative breast cancer is still a great challenge, and there is a need for new anticancer compounds to overcome its high drug resistance [6].

To overcome multidrug resistance (MDR) in cancer, several approaches have been proposed, mainly focused on the development of molecules that can act on MDR mechanisms. The deregulation of apoptosis and cell cycle pathways are among the most frequent alterations in cancer cells responsible for drug resistance and cancer development [7]. Apoptosis is characterized by a series of biochemical events that play a key role in the regulation of many physiological and pathophysiological processes. In drug-resistant cancer cells, the mechanisms of apoptosis are suppressed, causing an imbalance between cell death and proliferation [8,9]. Moreover, changes in the cell cycle regulatory signaling pathways are commonly altered in cancer cells, which often lose their checkpoint mechanisms, contributing to cell proliferation. Therefore, targeting deficient cell checkpoints and apoptosis are considered promising strategies for improving anticancer drug development and overcoming MDR [7,10].

Natural products have been an important source for the discovery of new bioactive compounds with anticancer properties. The most known clinically used chemotherapeutic agents for cancer treatment are from natural sources [11,12].

Plants from the Amaryllidaceae family are characterized by containing a wide range of unique and structurally diverse bioactive Amaryllidaceae-type alkaloids. Some of them have shown great anticancer activity, mainly lycorine [13,14].

In our search for new anticancer compounds targeting multidrug resistance in cancer, e.g., [15–23], recently, our group has reported a derivative of a monoterpene indole alkaloid isolated from the African medicinal plant *Tabernaemontana elegans* [24] that is shown to be highly effective against breast and ovarian cancer cells [25]. Aiming at finding new anticancer compounds against breast cancer cells, this study was conducted to obtain bioactive alkaloids from *Pancratium maritimum* L. (Amaryllidaceae family), which led to the isolation of nine Amaryllidaceae-type alkaloids, along with two other compounds.

The antiproliferative effect of compounds (1–11) was evaluated against the triple-negative breast cancer cell lines MDA-MB-231 and MDA-MB-466, the breast cancer MCF-7, and the non-malignant cell lines MCF-12A and HFF-1. Compound 7 was selected for further studies in MDA-MB-231 breast cancer cells to evaluate the mechanisms underlying its antiproliferative activity, namely the effect of the compound on cell cycle and apoptosis.

2. Results and Discussion

2.1. Isolation of Compounds

The bulbs of *P. maritimum* were exhaustively extracted with methanol. Subsequent acid-base portioning of the methanol extract, at different pH values (5 and 9) and organic solvents, yielded the alkaloid fractions, which were further fractionated by chromatographic methods, yielding several Amaryllidaceae-type alkaloids, bearing scaffolds of the haemanthamine-, homolycorine-, lycorine-, galanthamine-, and tazettine-type (3–11), namely the alkaloids haemanthidine (3) [13], hippeastrine (4) [13], lycorine (5) [13], 11 α -hydroxygalanthamine (6) [26], 2 α -10 β -dihydroxy-9-*O*-demethylhomolycorine (7) [27], epi-galanthamine (8) [13], 8-*O*-demethylhomolycorine (9) [13], tazettine (10) [13], and haemanthamine (11) [13]. The alkamide *N-trans*-feruloyl-tyramine (2) [28] and the phenolic compound 4,6-dimethoxy-2-hydroxy acetophenone (1) [29] were also isolated. The structures of the compounds (Figure 1) were established based on their spectroscopic data, mainly by 1D and 2D NMR and mass spectrometry (Supporting Information), which were in agreement with those reported in the literature for these compounds.

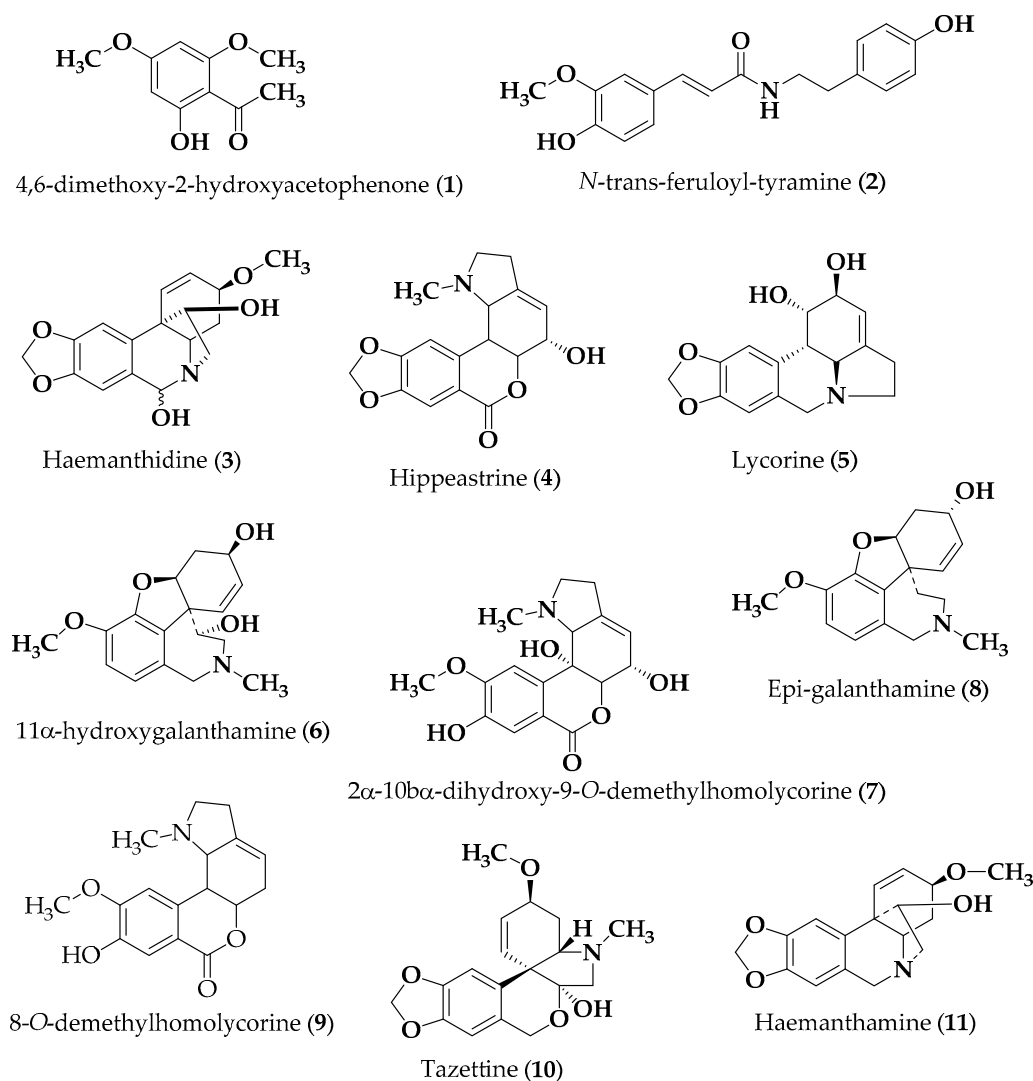


Figure 1. Chemical structures of compounds 1–11.

2.2. Biological Activity

2.2.1. Antiproliferative Effect Evaluation

The antiproliferative effect of the isolated compounds (1–11) was investigated by the sulforhodamine B assay against human triple-negative breast cancer cell lines (MDA-MB-468 and MDA-MB-231) and breast ductal carcinoma cells (MCF-7) and the non-tumorigenic fibroblast (HFF-1) and breast cell lines (MCF12A). The IC_{50} values were determined after 48 h of treatment (Table 1).

Lycorine (5) was found to be the most effective compound against the three breast cancer cell lines, exhibiting the lowest IC_{50} values (0.92 and 1.42 μ M in the triple-negative cancer cells, MDA-MB-231 and MDA-MB-468, respectively; IC_{50} of 0.73 μ M in the MCF-7 breast cancer cell line). Similarly, compounds 3 and 11 also showed strong growth inhibitory effects against MDA-MB-231 cells (4.88 and 3.95 μ M, respectively), MDA-MB-468 (IC_{50} of 3.5 and 3.8 μ M, respectively), and MCF-7 cell lines (IC_{50} of 2.7 and 1.6 μ M, respectively). Similarly, a pronounced antiproliferative activity was also found for compound 7 against MDA-MB-231 cells (IC_{50} of 8.02 μ M) and MCF-7 (IC_{50} of 6.8 μ M), whereas a higher IC_{50} value of 16. A total of 3 μ M was obtained in MDA-MB-468 cells. Interestingly, compound 7 displayed much higher activity than its structurally related compounds, 4 (IC_{50} of 24.70 μ M) and 9 (IC_{50} > 40), suggesting that the higher number of free hydroxyl groups found in compound 7 may explain this different activity between the three compounds.

In addition, the antiproliferative effect of the compounds was evaluated on the non-malignant fibroblast (HFF-1) and breast (MCF12A) cell lines. When comparing the IC₅₀ values obtained in HFF-1 cells with those obtained in cancer cell lines, a slight selectivity (SI) was found for compound **7** in MDA-MB-231 (SI of 1.65) and MCF-7 (SI of 2.37) cancer cells. Conversely, compounds **5** and **11** exhibited slight selectivity in all breast cancer cell lines in relation to MCF12A cells, particularly compound **5** against MDA-MB-231 cells (SI of 3.26) and both **5** and **11** in MCF-7 cells (SI of over 4).

In previous studies, compounds **3**, **5**, and **11** have shown antiproliferative activity against MDA-MB-231 breast cancer cells, which is in agreement with our results [30].

Table 1. Effect of compounds **1–11** on the growth in a panel of human breast cancer (triple negative MDA-MB-231 and MDA-MB-466 cell lines, and MCF-7 cells) and non-tumorigenic fibroblast (HFF-1 and breast (MCF12A)) cell lines.

Compounds/ Cell Line	IC ₅₀ (μM) ^a					SI ^b					
	MDA-MDB- 231 (A)	MDA-MB- 468 (B)	MCF-7 (C)	MCF12A (D)	HFF-1 (E)	D/A	D/B	D/C	E/A	E/B	E/C
1	>40	-	-	-	-	-	-	-	-	-	-
2	>40	-	-	-	-	-	-	-	-	-	-
3	4.9 ± 1.16	3.5 ± 0.3	2.7 ± 0.1	5.0 ± 0.5	2.7 ± 0.15	1.02	1.42	1.85	0.56	0.78	1.01
4	24.7 ± 4.30	-	-	-	-	-	-	-	-	-	-
5	0.9 ± 0.20	1.4 ± 0.01	0.7 ± 0.01	3.0 ± 0.3	1.3 ± 0.30	3.26	2.11	4.10	1.41	0.91	1.78
6	>40	-	-	-	-	-	-	-	-	-	-
7	8.0 ± 1.68	16.3 ± 1.3	6.8 ± 0.2	5.6 ± 0.8	13.3 ± 3.28	0.69	0.34	0.82	1.65	0.81	2.37
8	>40	-	-	-	-	-	-	-	-	-	-
9	>40	-	-	-	-	-	-	-	-	-	-
10	39.0 ± 1.41	-	-	-	-	-	-	-	-	-	-
11	3.9 ± 0.97	3.8 ± 0.4	1.6 ± 0.1	6.5 ± 1.1	2.7 ± 0.72	1.64	1.71	4.06	0.68	0.71	1.7
Etoposide	2.9 ± 0.1	1.7 ± 0.05	3.1 ± 0.05	2.3 ± 0.13	3.8 ± 0.09	0.79	1.35	0.74	1.31	2.23	1.23

^a IC₅₀ values were determined by sulforhodamine B assay after 48 h of treatment (growth obtained with the vehicle was set as 100%). Data are mean ± SEM of four to six independent experiments. ^b SI: Selectivity index; SI < 1 values denote lack of selectivity, 1 < SI < 3 mean slight selectivity and are marked with bold and italics; 3 < SI < 6 values indicate moderate selectivity and are highlighted in bold, whereas values of SI > 6 indicate that compounds are strongly selective [31]. Etoposide was used as a positive control.

2.2.2. Analysis of Cell Cycle, Apoptosis, and Mitochondrial ROS Generation

Compound **7**, the antiproliferative effect of which has not been investigated yet, was selected for further studies in the triple-negative breast cancer cell line MDA-MB-231.

To explore the ability of compound **7** to regulate cell cycle progression, the percentage of cells in different phases was analyzed after 24 h of exposure. As shown in Figure 2B, a two-fold IC₅₀ concentration of compound **7** (16 μM) induced a significant accumulation of cells in the G2/M phase compared to the vehicle control cells. Importantly, at 16 μM, compound **7** did not significantly interfere with cell cycle, cell death, and mitochondrial ROS generation in HFF-1 cells.

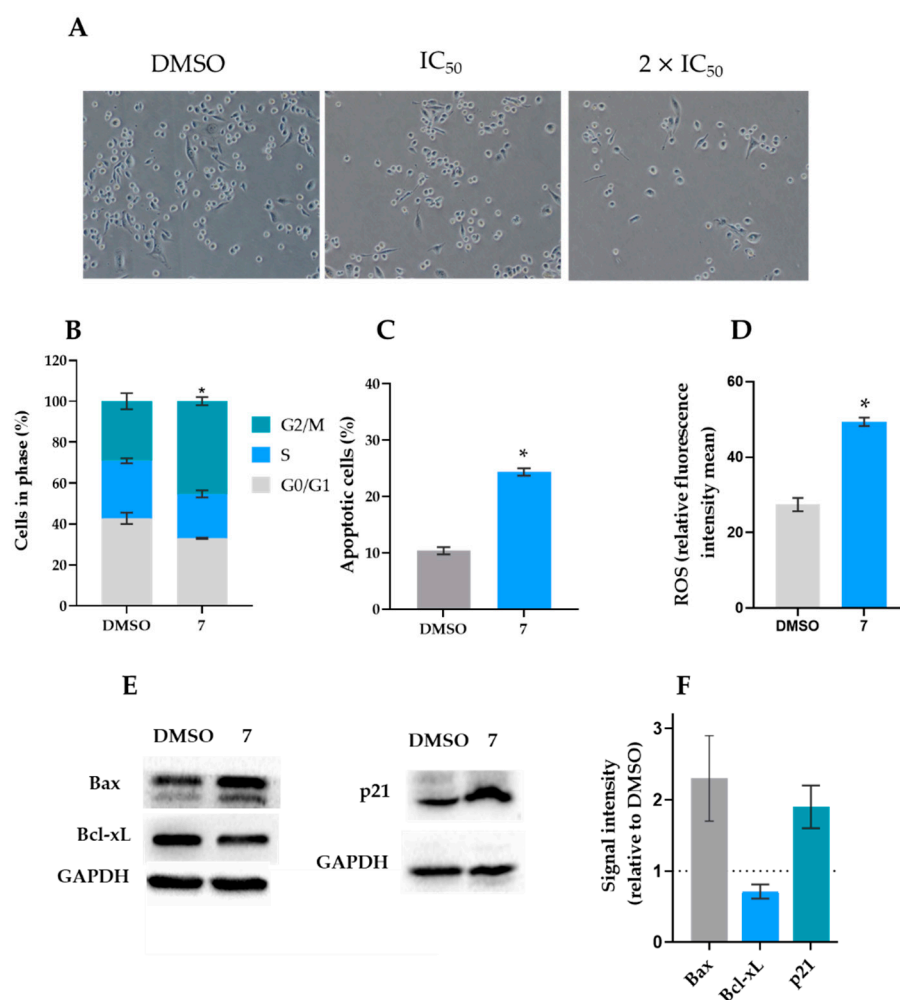


Figure 2. Compound 7 induced cell cycle arrest, apoptosis, and ROS production, in MDA-MB-231 cells. (A) Effect of 8 (IC_{50}) and 16 ($2 \times IC_{50}$) μM of compound 7 on MDA-MB-231 cell cytotoxicity after 48 h of treatment. (B) Effect of 16 μM of compound 7 on cell cycle progression after 48 h of treatment in MDA-MB-231 cells; the percentage of cells in each phase of the cell cycle was analyzed by flow cytometry, using PI; data are mean \pm SEM of three independent experiments. Values are significantly different from DMSO (* $p < 0.05$, unpaired Student's t -test). (C) Effect of 16 μM of compound 7 on apoptosis after 48 h of treatment; the percentage of Annexin-positive cells was analyzed by flow cytometry using PI and Annexin-V staining; data are mean \pm SEM of three independent experiments. Values are significantly different from DMSO (* $p < 0.05$, unpaired Student's t -test). (D) Effect of 16 μM of compound 7 on mitochondrial ROS generation after 24 h of treatment; data are mean \pm SEM of three independent experiments (* $p < 0.05$, unpaired Student's t -test). (E) Effect of 16 μM of compound 7 after 48 h of treatment on the protein expression levels in MDA-MB-231 cells. Immunoblots are representative of three independent experiments. GAPDH was used as a loading control. (F) The graph represents the quantification of protein expression levels relative to DMSO; data are mean \pm SD of three independent experiments. The ability of compound 7 to induce apoptosis in this cell line was also assessed by cytometry, using the Annexin V-FITC assay after 48 h of treatment. Apoptosis is characterized by distinct morphologic features. In the early stages of apoptosis, the membrane phospholipid phosphatidylserine is translocated from the inner to the outer plasma membrane leaflet. Annexin V is a phospholipid-binding protein with a high affinity to phosphatidylserine, which is able to detect apoptotic cells with the externalization of phosphatidylserine [32]. The results showed a significant increase in the percentage of apoptotic cells in MDA-MB-231 cells compared to the vehicle control after treatment with 16 μM of compound 7 (Figure 2C). In line with this, it was further observed that 16 μM of compound 7 increased ROS production in MDA-MB-231 cells (Figure 2D).

2.2.3. Western Blot Analyses

Once compound 7 induced cancer cell death by apoptosis, we next explored the molecular pathways involved in its apoptotic effect. For that, some apoptotic-related proteins were checked in MDA-MB-231 cells treated with 16 μM of compound 7 for 48 h (Figure 2E,F). The results showed increased levels of the pro-apoptotic protein Bax and reduced levels of the anti-apoptotic Bcl-xL, thus substantiating the data obtained in the Annexin V-FITC assay. Nonetheless, the compound did not interfere with the p53 protein expression levels (data not shown).

Moreover, in accordance with induction of a G2/M cycle arrest, compound 7 also increased the p21 protein levels.

2.2.4. Combination Therapy

To evaluate the ability of compound 7 of promoting the anticancer effect of conventional chemotherapeutic drugs, MDA-MB-231 cells were treated with a single concentration of compound 7 (at 1.5 μM ; concentration with no significant effect on cancer cell growth) in combination with a DNA-damaging agent, such as etoposide. The results showed that 1.5 μM of compound 7 significantly increased the growth inhibitory effect of etoposide at the concentrations of 0.8, 1.5, and 3 μM (Figure 3). A multiple drug-effect analysis was carried out for each combination, with the calculation of the combination index (CI), which revealed synergistic effects between compound 7 and 0.8, 1.5, and 3 μM of etoposide (Table 2). Of note, for the same experimental conditions used in MDA-MB-231 cells, no synergistic effects were observed in HFF-1 cells (Table 2).

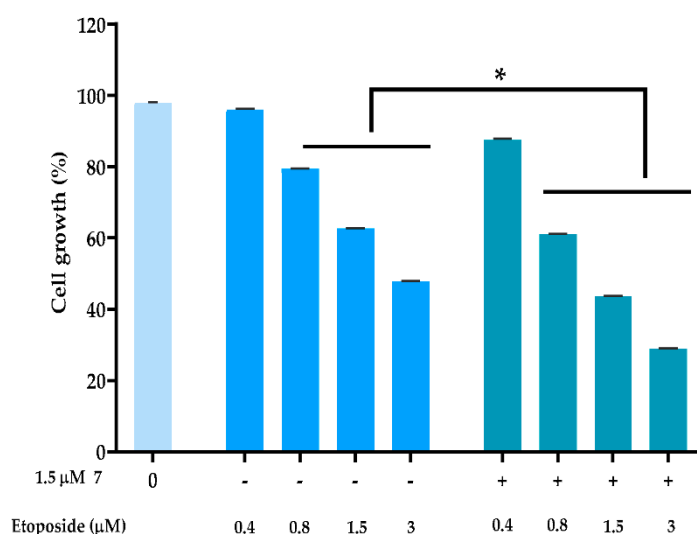


Figure 3. Compound 7 sensitized MDA-MB-231 cells to the effect of etoposide. Cells were treated with a range of concentrations of the conventional chemotherapeutic drug alone and in combination with 1.5 μM of compound 7; cell proliferation was measured after 48 h of treatment; the growth obtained with control (DMSO) was set as 100%; data are mean \pm SEM; values significantly different from chemotherapeutic drug alone: * $p < 0.05$ (two-way ANOVA followed by Sidak's test).

Table 2. Effect of compound 7 in combination with etoposide, in MDA-MB-231 and HFF-1 cells.

Combination with Etoposide (μM)	Combination Index	
	MDA-MB-231	HFF-1
0.4	1.23	1.19
0.8	0.87	1.34
1.5	0.81	1.12
3	0.86	1.09

The effect of 1.5 μM of compound 7 in combination with a range of concentrations of etoposide was evaluated after 48 h of treatment using CompuSyn software to calculate the combination index (CI) values for each combined treatment: $\text{CI} < 1$, synergy; $1 < \text{CI} < 1.1$, additive effect; $\text{CI} > 1.1$, antagonism.

3. Materials and Methods

3.1. General Experimental Procedure

The NMR spectra were recorded on a Bruker 300 Ultra-Shield instrument (^1H 300 MHz, ^{13}C 75 MHz). ^1H and ^{13}C chemical shifts are expressed in δ (ppm) referenced to the solvent used and the proton coupling constants J are in hertz (Hz). Optical rotations were performed using a PerkinElmer 241 polarimeter, with quartz cells of 1 dm path length. The infrared spectra were collected on an Affinity-1 (Shimadzu, Kyoto, Japan) FTIR spectrophotometer. Low-resolution mass spectrometry was conducted with a Triple Quadrupole mass spectrometer Waters AcquityTM (Waters[®], Ireland). Column chromatography (CC) was performed on silica gel (Merck 9385, Darmstadt, Germany) or Combiflash system (teledyne-Isco; Lincoln, NE, USA), using SiO_2 or C_{18} prepacked columns. Analytical thin-layer chromatography (TLC) was performed on pre-coated silica gel 60 F₂₅₄ and RP-18 F₂₅₄ plates (Merck 105,554 and 105,560, respectively), with visualization under UV light (λ 254 and 366 nm), and by spraying either with Dragendorff's reagent or a solution of H_2SO_4 -MeOH (1:1), followed by heating.

3.2. Plant Material

The whole plant of *Pancreatium maritimum* was collected in August 2018, during the flowering period, at Cabo Raso, Cascais, Portugal. The plant was identified by Dr. Teresa Vasconcelos (plant taxonomist) of Instituto Superior de Agronomia, Technical University of Lisbon, Portugal. A voucher specimen (no. LISI044123) has been deposited at the herbarium João de Carvalho Vasconcellos of Instituto Superior de Agronomia.

3.3. Tested Compounds

The chemical structures of compounds are presented in Figure 1. These included 4,6-dimethoxy-2-hydroxyacetophenone (1), *N*-trans-feruloyl-tyramine (2), haemanthidine (3), hippastrine (4), lycorine (5), 11 α -hydroxygalanthamine (6), 2 α -10 α -dihydroxy-9-*O*-demethylhomolycorine (7), epi-galanthamine (8), 9-*O*-demethylhomolycorine (9), tazettine (10), and haemanthamine (11). The isolation of compounds is described below. Etoposide was obtained from Sigma-Aldrich (Sintra, Portugal). All tested compounds were dissolved in dimethyl sulfoxide (DMSO) from Sigma-Aldrich (Sintra, Portugal). In all experiments, the solvent (0.1–0.25% DMSO) was included as a control.

3.4. Extraction and Isolation

The fresh bulbs (14.8 kg) of *P. maritimum* were sliced, dried at 40 °C for 48 h, and then minced. The resulting powder (8.19 kg) was extracted with MeOH (11 \times 30 L). Afterward, the crude methanol extract (1.034 kg) was suspended in a solution of HCl 2% (*v/v*; 2.0 L), and the neutral material was removed with Et_2O (3 \times 1 L). The pH of the aqueous phase was adjusted to 5 by the addition of dilute NH_4OH and successively extracted with CH_2Cl_2 (3 \times 500 mL), EtOAc (4 \times 1 L), and *n*-butanol (4 \times 1 L), yielding, after drying over anhydrous Na_2SO_4 and evaporating the solvents under reduced pressure, the CH_2Cl_2 _{pH5} (13.9 g) and EtOAc_{pH5} (20 g) and the *n*-butanol_{pH5} (109 g)-soluble fractions. Then, the pH of the aqueous phase was adjusted to 9, by adding NH_4OH , and extracted again with EtOAc (3 \times 1 L) and *n*-butanol (4 \times 1 L), originating two new alkaloid fractions after the above procedure (EtOAc_{pH9} 10.3 g; and *n*-butanol_{pH9} 32.2 g) (see Figure S1 and Table S1, Supplementary Materials).

The residue of the powdered bulbs was further extracted with MeOH using a Soxhlet apparatus (500 g each dose for 10 h). The resulting MeOH extract (168 g) was submitted to

acid-base extraction, as described above, yielding the EtOAc_{pH9} (3.5 g) and *n*-butanol_{pH9} (4.5 g)-soluble fractions (see Table S1, Supplementary Materials).

The alkaloid CH₂Cl₂_{pH5} (13.9g) and EtOAc_{pH5} (20g)-soluble fractions have shown the same chromatographic profile (TLC) and were combined, and then fractionated over silica gel column chromatography (*n*-hexane–EtOAc, 9:1 to 0:1; EtOAc–MeOH, 1:0 to 3:2). Column chromatography of a fraction eluted with *n*-hexane–EtOAc (4:1; 489 mg) (*n*-hexane–CH₂Cl₂, 1:0 to 7:3), on silica gel, yielded compound **1** (122 mg), whereas compound **2** (17 mg) was obtained by repeated column chromatography, on silica gel, of a fraction eluted with *n*-hexane–EtOAc (1:4; 3.94 g), using mixtures of CH₂Cl₂/MeOH (1:0 to 7:3), followed by preparative TLC (CH₂Cl₂/MeOH, 9:1). The alkaloid soluble fraction BuOH_{pH5} (109 g) was subjected to silica gel column chromatography, using solvent mixtures of increasing polarity (*n*-hexane–CH₂Cl₂, 0:1; CH₂Cl₂–MeOH, 1:0 to 7:3). Column chromatography of a fraction eluted with CH₂Cl₂–MeOH (9:1; 19.9 g) on silica gel (*n*-hexane–CH₂Cl₂, 1:0 to 0:1), followed by purification by Combiflash (80 g prepacked SiO₂ column, RediSep[®] Rf, Teledyne Isco, Lincoln, NE, USA), using as the eluent *n*-hexane–EtOAc (1:0 to 0:1, 5% increments with an 8 mL·min^{−1}), yielded compounds **3** (3.595 g) and **4** (15 mg).

In turn, compound **5** (1.2 g) was obtained through crystallization with methanol of the crude alkaloid fraction EtOAc_{pH9} (10.3 g). Further study of the mother liquid of this fraction, by repeated column chromatography (*n*-hexane–EtOAc, 7:3 to 0:1 and EtOAc–MeOH, 0:1 to 1:0; CH₂Cl₂/MeOH 1:0 to 3:7) afforded compound **6** (155 mg), after further purification by crystallization (*n*-hexane–EtOAc). Crystallization of the fraction eluted with EtOAc–MeOH (7:3; 790 mg) from methanol led to the isolation of compound **7** (97 mg). The resulting mother liquid was fractionated on silica gel (*n*-hexane–EtOAc, 7:3 to 0:1; EtOAc–MeOH, 1:0 to 7:3) to yield a fraction (280 mg) that was chromatographed on aluminum oxide (CH₂Cl₂–MeOH, 1:0 to 1:9), followed by preparative TLC (CH₂Cl₂/MeOH, 19:1), affording compounds **8** (30 mg) and **9** (7 mg).

The alkaloid soluble fraction BuOH_{pH9} (32.2 g) was fractionated over aluminum oxide (CH₂Cl₂–MeOH, 1:0 to 0:1) to yield several fractions. The fraction eluted with CH₂Cl₂–MeOH (19:1; 446 mg) was crystallized from MeOH to obtain 77 mg of the previously isolated compound **5**. The resulting mother liquid was submitted to silica gel chromatography (CH₂Cl₂–MeOH, 1:0 to 9:1) to afford compound **10** (20 mg).

Concerning the Soxhlet extract, the crystallization of EtOAc_{pH9} fraction (3.53 g) with methanol led to the isolation of compound **5** again (400 mg). Successive fractionation of the mother liquid on silica gel, first with *n*-hexane–EtOAc (1:0 to 0.1) and EtOAc–MeOH (1:0 to 7:3), and after with CH₂Cl₂/MeOH (1:0 to 9:1), afforded compound **11** (8 mg).

3.5. Human Cell Lines and Growth Conditions

Human breast adenocarcinoma MDA-MB-231, MDA-MB-468, and MCF-7 cell lines and non-tumorigenic foreskin fibroblast (HFF-1) and breast (MCF12A) cell lines were purchased from American Type Culture Collection (ATCC, Rockville, MD, USA). All cancer cell lines, except MCF12A, were routinely cultured in RPMI-1640 medium with glutamine from Corning (VWR, Carnaxide, Portugal) supplemented with 10% fetal bovine serum (FBS) from Biowest (Labclinics, Barcelona, Spain). MCF12A cells were cultured in a 1:1 mixture of Dulbecco's modified Eagle's medium and Ham's F12 medium, 20 ng/mL human epidermal growth factor, 100 ng/mL cholera toxin, 0.01 mg/mL bovine insulin, and 500 ng/mL hydrocortisone and supplemented with 10% FBS. All cells were maintained in a humidified incubator at 37 °C with 5% CO₂. All cells were routinely tested for mycoplasma contamination using the MycoAlert[™] PLUS detection kit (Lonza, Basel, Switzerland).

3.6. Sulforhodamine B Assay

Human cell lines were seeded in 96-well plates at a density of 5.0×10^3 (MDA-MB-231, MCF-7, HFF-1, and MCF12A) and 7.5×10^3 (MDA-MB-468) cells/well and allowed to adhere for 24 h. Cells were treated with serial dilutions of compounds (ranging from 0.1 to 40 μM) for an additional 48 h. Effect on cell proliferation was measured by sulforhodamine

B assay, as described in [33], and the half-maximal inhibitory concentration (IC_{50}) was then determined for each cell line using the GraphPad Prism software version 7.0 (La Jolla, CA, USA).

3.7. Cell Cycle and Apoptosis Analysis

The analyses were performed basically as described in [33]. Briefly, MDA-MB-231 cells were seeded in 6-well plates at a density of 1.5×10^5 cells/well for 24 h, followed by treatment with 16 μ M of compound 7 for an additional 48 h. For cell cycle analysis, cells were stained with propidium iodide (PI; Sigma-Aldrich, St. Louis, MO, USA). The cells were then analyzed by flow cytometry, and cell cycle phases were identified and quantified using the FlowJo \times 10.0.7 Software (Treestar, Ashland, OR, USA). For apoptosis, cells were stained using the Annexin V-FITC Apoptosis Detection Kit I from BD Biosciences (Enzifarma, Porto, Portugal), according to the manufacturer's instructions. The AccuriTM C6 flow cytometer and the BD Accuri C6 software (BD Biosciences) were used.

3.8. Mitochondrial Reactive Oxygen Species (ROS) Generation

For mitochondrial ROS generation assessment, MDA-MB-231 cells were seeded in 6-well plates at a density of 1.5×10^5 cells/well for 24 h, followed by treatment with 16 μ M of compound 7 for an additional 24 h. Thereafter, cells were incubated with 3 μ M MitoSOX (Thermo Fisher Scientific, Invitrogen, Portugal) for 30 min at 37 °C and analyzed by flow cytometry.

3.9. Western Blot Analysis

MDA-MB-231 cells were seeded in 6-well plates at a density of 1.5×10^5 cells/well for 24 h, followed by treatment with 16 μ M of compound 7. Protein extracts were quantified using the Bradford reagent (Sigma-Aldrich). Proteins were run in SDS-PAGE and transferred to a Whatman nitrocellulose membrane from Protan (VWR, Carnaxide, Portugal). After blocking, proteins were identified using specific primary antibodies: rabbit polyclonal anti-p21 (Santa Cruz Biotechnology, Dallas, TX, USA), rabbit polyclonal anti-Bax, and rabbit monoclonal anti-Bcl-xL (Invitrogen, Waltham, MA, USA), followed by the respective anti-mouse/anti-rabbit HRP-conjugated secondary antibodies (Santa Cruz Biotechnology). GAPDH was used as a loading control. The signal was detected with the ECL Amersham kit from GE Healthcare (VWR, Carnaxide, Portugal). Two detection methods were used: the Kodak GBX developer and fixer (Sigma-Aldrich) or the ChemiDocTM XRS Imaging System from Bio-Rad Laboratories (Amadora, Portugal).

3.10. Combination Therapy Assays

To assess the synergistic effect of compound 7 with the conventional chemotherapeutic drug etoposide, MDA-MB-231 cells were treated with compound 7 at 1.5 μ M (concentration that did not interfere with the growth of cancer cells) and/or increasing concentrations of etoposide, for 48 h. The effect of combined treatments on cell proliferation was analyzed by SRB assay. For each combination, the combination index (CI) values were calculated using the CompuSyn Software version 1.0; CI values < 1 , $1 < CI < 1.1$, and > 1.1 indicate synergistic, additive, and antagonistic effects, respectively [34].

3.11. Statistical Analysis

The data were analyzed statistically using the GraphPad Prism (La Jolla, CA, USA; version 8.0.2) software for Microsoft Windows 10. For the comparison of the two groups, the unpaired Student's *t*-test was used. For the comparison of multiple groups, the two-way ANOVA followed by Sidak's test was used. Statistical significance was set as $* p < 0.05$.

4. Conclusions

To summarize, among the nine Amaryllidaceae-type alkaloids isolated from *P. maritimum*, bearing different scaffolds, the most significant growth inhibitory activity against

different human breast cancer cell lines was found for compounds **3**, **5**, **7**, and **11**. When comparing the IC₅₀ values obtained for compound **7** with those of **4** and **9**, sharing the same homolycorine-type scaffold, the higher number of hydroxyl groups in compound **7** seems to be associated with its higher activity. Further investigation of the mechanism of action of compound **7** against the triple-negative human breast cancer MDA-MB-231 cell line revealed that its antiproliferative effect was associated with the induction of apoptosis and cell cycle arrest through a p53-independent pathway. Interestingly, compound **7** seems to interfere with the expression levels of proteins of the Bcl-2 family, namely increasing Bax and reducing Bcl-xL, which may indicate a potential involvement of the mitochondrial pathway in its antitumor activity. In fact, an increase in mitochondrial ROS production was also observed upon compound **7** treatment. The results obtained in this work also revealed that triple-negative breast cancer therapy might greatly benefit from the combination of etoposide with compound **7**.

Supplementary Materials: The following supporting information can be downloaded at: <https://www.mdpi.com/article/10.3390/molecules27185759/s1>, Figure S1: Extraction and fractionation of the methanol extract of *P. maritimum* and the isolated compounds (**1–11**); Table S1: Fractions obtained from acid–base extraction; Figure S2–Figure S17: spectroscopic data of the isolated compounds; NMR data of some compounds.

Author Contributions: All the authors made significant contributions to the manuscript. M.J.U.F. designed and supervised the study; L.S. supervised the biological assays.; S.A.R.S. performed the phytochemical study; A.V.G. and J.B.L. performed the biological assays; S.A.R.S. and M.J.U.F. wrote the manuscript; All authors have read and agreed to the published version of the manuscript.

Funding: This research was funded by Fundação para a Ciência e Tecnologia (FCT), Portugal (Projects PTDC/MED-QUI/30591/2017, UIDB/50006/2020, and Ph.D. grant SFRH/BD/130348/2017). The NMR spectrometers are part of the National NMR Network (PTNMR) and are partially supported by Infrastructure Project no 022161 (co-financed by FEDER through COMPETE 2020, POCI and PORL, and FCT through PIDDAC).

Institutional Review Board Statement: Not applicable.

Informed Consent Statement: Not applicable.

Data Availability Statement: The data that support the findings of this study are available from the corresponding author upon request.

Conflicts of Interest: The authors declare no conflict of interest.

References

1. Ferlay, J.; Colombet, M.; Soerjomataram, I.; Parkin, D.M.; Piñeros, M.; Znaor, A.; Bray, F. Cancer Statistics for the Year 2020: An Overview. *Int. J. Cancer* **2021**, *149*, 778–789. [[CrossRef](#)] [[PubMed](#)]
2. Wu, T.-N.; Chen, H.-M.; Shyur, L.-F. Current Advancements of Plant-Derived Agents for Triple-Negative Breast Cancer Therapy through Deregulating Cancer Cell Functions and Reprogramming Tumor Microenvironment. *Int. J. Mol. Sci.* **2021**, *22*, 13571. [[CrossRef](#)] [[PubMed](#)]
3. Singh, S.; Numan, A.; Maddiboyina, B.; Arora, S.; Riadi, Y.; Md, S.; Alhakamy, N.A.; Kesharwani, P. The Emerging Role of Immune Checkpoint Inhibitors in the Treatment of Triple-Negative Breast Cancer. *Drug Discov. Today* **2021**, *26*, 1721–1727. [[CrossRef](#)] [[PubMed](#)]
4. Han, Y.; Yu, X.; Li, S.; Tian, Y.; Liu, C. New Perspectives for Resistance to PARP Inhibitors in Triple-Negative Breast Cancer. *Front. Oncol.* **2020**, *10*, 1–14. [[CrossRef](#)] [[PubMed](#)]
5. Nedeljković, M.; Damjanović, A. Mechanisms of Chemotherapy Resistance in Triple-Negative Breast Cancer—How We Can Rise to the Challenge. *Cells* **2019**, *8*, 957. [[CrossRef](#)]
6. Chen, H.; Yang, J.; Yang, Y.; Zhang, J.; Xu, Y.; Lu, X. The Natural Products and Extracts: Anti-Triple-Negative Breast Cancer in Vitro. *Chem. Biodivers.* **2021**, *18*, e2001047. [[CrossRef](#)]
7. Majidinia, M.; Mirza-Aghazadeh-Attari, M.; Rahimi, M.; Mihanfar, A.; Karimian, A.; Safa, A.; Yousefi, B. Overcoming Multidrug Resistance in Cancer: Recent Progress in Nanotechnology and New Horizons. *IUBMB Life* **2020**, *72*, 855–871. [[CrossRef](#)]
8. Pavlíková, L.; Šereš, M.; Breier, A.; Sulová, Z. The Roles of MicroRNAs in Cancer Multidrug Resistance. *Cancers* **2022**, *14*, 1090. [[CrossRef](#)]

9. Neophytou, C.M.; Trougakos, I.P.; Erin, N.; Papageorgis, P. Apoptosis Deregulation and the Development of Cancer Multi-Drug Resistance. *Cancers* **2021**, *13*, 4363. [[CrossRef](#)]
10. Sun, Y.; Liu, Y.; Ma, X.; Hu, H. The Influence of Cell Cycle Regulation on Chemotherapy. *Int. J. Mol. Sci.* **2021**, *22*, 6923. [[CrossRef](#)]
11. Newman, D.J.; Cragg, G.M. Natural Products as Sources of New Drugs over the Nearly Four Decades from 01/1981 to 09/2019. *J. Nat. Prod.* **2020**, *83*, 770–803. [[CrossRef](#)] [[PubMed](#)]
12. Agarwal, G.; Carcache, P.J.B.; Addo, E.M.; Kinghorn, A.D. Current Status and Contemporary Approaches to the Discovery of Antitumor Agents from Higher Plants. *Biotechnol. Adv.* **2020**, *38*, 107337. [[CrossRef](#)] [[PubMed](#)]
13. Bastida, J.; Lavilla, R.; Viladomat, F. Chemical and Biological Aspects of Narcissus Alkaloids. In *The Alkaloids*; Cordell, G.A., Ed.; Elsevier: Amsterdam, The Netherlands, 2006; Volume 63, pp. 87–179.
14. Cedrón, J.C.; Del Arco-Aguilar, M.; Estévez-Braun, A.; Ravelo, Á.G. Chemistry and Biology of Pancreatic Alkaloids. In *The Alkaloids*; Cordell, G.A., Ed.; Academic Press: Chennai, India, 2010; Volume 68, pp. 1–37.
15. Cardoso, D.S.P.; Kincses, A.; Nové, M.; Spengler, G.; Mulhovo, S.; Aires-de-Sousa, J.; dos Santos, D.J.V.A.; Ferreira, M.J.U. Alkylated Monoterpene Indole Alkaloid Derivatives as Potent P-Glycoprotein Inhibitors in Resistant Cancer Cells. *Eur. J. Med. Chem.* **2021**, *210*, 112985. [[CrossRef](#)] [[PubMed](#)]
16. Cardoso, D.S.P.; Szemerédi, N.; Spengler, G.; Mulhovo, S.; Dos Santos, D.J.V.A.; Ferreira, M.J.U. Exploring the Monoterpene Indole Alkaloid Scaffold for Reversing P-Glycoprotein-Mediated Multidrug Resistance in Cancer. *Pharmaceuticals* **2021**, *14*, 862. [[CrossRef](#)]
17. Ferreira, R.J.; Baptista, R.; Moreno, A.; Madeira, P.G.; Khonkarn, R.; Baubichon-Cortay, H.; Dos Santos, D.J.; Falson, P.; Ferreira, M.J.U. Optimizing the Flavanone Core toward New Selective Nitrogen-Containing Modulators of ABC Transporters. *Future Med. Chem.* **2018**, *10*, 725–741. [[CrossRef](#)] [[PubMed](#)]
18. Ferreira, R.J.; Gajdács, M.; Kincses, A.; Spengler, G.; dos Santos, D.J.V.A.; Ferreira, M.J.U. Nitrogen-Containing Naringenin Derivatives for Reversing Multidrug Resistance in Cancer. *Bioorg. Med. Chem.* **2020**, *28*, 115798. [[CrossRef](#)]
19. Paterna, A.; Kincses, A.; Spengler, G.; Mulhovo, S.; Molnár, J.; Ferreira, M.J.U. Dregamine and Tabernaemontanine Derivatives as ABCB1 Modulators on Resistant Cancer Cells. *Eur. J. Med. Chem.* **2017**, *128*, 247–257. [[CrossRef](#)]
20. Paterna, A.; Khonkarn, R.; Mulhovo, S.; Moreno, A.; Madeira, P.G.; Baubichon-Cortay, H.; Falson, P.; Ferreira, M.J.U. Monoterpene Indole Alkaloid Azine Derivatives as MDR Reversal Agents. *Bioorg. Med. Chem.* **2018**, *26*, 421–434. [[CrossRef](#)]
21. Reis, M.A.; Ahmed, O.B.; Spengler, G.; Molnár, J.; Lage, H.; Ferreira, M.J.U. Jatrophone Diterpenes and Cancer Multidrug Resistance-ABCB1 Efflux Modulation and Selective Cell Death Induction. *Phytomedicine* **2016**, *23*, 968–978. [[CrossRef](#)]
22. Reis, M.A.; Matos, A.M.; Duarte, N.; Ahmed, O.B.; Ferreira, R.J.; Lage, H.; Ferreira, M.J.U. Epoxyalthyrane Derivatives as MDR-Selective Compounds for Disabling Multidrug Resistance in Cancer. *Front. Pharmacol.* **2020**, *11*, 1–11. [[CrossRef](#)]
23. Ramalheite, C.; Mulhovo, S.; Lage, H.; Ferreira, M.J.U. Triterpenoids from *Momordica Balsamina* with a Collateral Sensitivity Effect for Tackling Multidrug Resistance in Cancer Cells. *Planta Med.* **2018**, *84*, 1372–1379. [[CrossRef](#)] [[PubMed](#)]
24. Paterna, A.; Borrallho, P.M.; Gomes, S.E.; Mulhovo, S.; Rodrigues, C.M.P.; Ferreira, M.J.U. Monoterpene Indole Alkaloid Hydrazone Derivatives with Apoptosis Inducing Activity in Human HCT116 Colon and HepG2 Liver Carcinoma Cells. *Bioorg. Med. Chem. Lett.* **2015**, *25*, 3556–3559. [[CrossRef](#)]
25. Raimundo, L.; Paterna, A.; Calheiros, J.; Ribeiro, J.; Cardoso, D.S.P.; Piga, I.; Neto, S.J.; Hegan, D.; Glazer, P.M.; Indraccolo, S.; et al. BBT20 Inhibits Homologous DNA Repair with Disruption of the BRCA1–BARD1 Interaction in Breast and Ovarian Cancer. *Br. J. Pharmacol.* **2021**, *178*, 3627–3647. [[CrossRef](#)] [[PubMed](#)]
26. Wildman, W.C.; Brown, C.L. The Structure of Habranthine. *Tetrahedron Lett.* **1968**, *9*, 4573–4576. [[CrossRef](#)]
27. Carvalho, K.R.; Silva, A.B.; Torres, M.C.M.; Pinto, F.C.L.; Guimarães, L.A.; Rocha, D.D.; Silveira, E.R.; Costa-Lotufo, L.V.; Braz-Filho, R.; Pessoa, O.D.L. Cytotoxic Alkaloids from *Hippeastrum Solandriiflorum* Lindl. *J. Braz. Chem. Soc.* **2015**, *26*, 1976–1980.
28. Fukuda, N.; Yonemitsu, M.; Kimura, T. Studies on the Constituents of the Stems of *Tinospora Tuberculata* N-Trans and N-Cis-Feruloyl Tyramine, and a New Phenolic Glucoside Tinotuberide. *Chem. Pharm. Bull.* **1983**, *31*, 156–161. [[CrossRef](#)]
29. Youssef, D.T.A.; Ramadan, M.A.; Khalifa, A.A. Acetophenones, a Chalcone, a Chromone and Flavonoids from *Pancreaticum Maritimum*. *Phytochemistry* **1998**, *49*, 2579–2583. [[CrossRef](#)]
30. Havelek, R.; Muthna, D.; Tomsik, P.; Kralovec, K.; Seifrtova, M.; Cahlikova, L.; Hostalkova, A.; Safratova, M.; Perwein, M.; Cermakova, E.; et al. Anticancer Potential of Amaryllidaceae Alkaloids Evaluated by Screening with a Panel of Human Cells, Real-Time Cellular Analysis and Ehrlich Tumor-Bearing Mice. *Chem. Biol. Interact.* **2017**, *275*, 121–132. [[CrossRef](#)]
31. Acton, E.M.; Narayanan, V.L.; Risbood, P.A.; Shoemaker, R.H.; Vistica, D.T.; Boyd, M.R. Anticancer Specificity of Some Ellipticinium Salts against Human Brain Tumors in Vitro. *J. Med. Chem.* **1994**, *37*, 2185–2189. [[CrossRef](#)]
32. Chen, T. *A Practical Guide to Assay Development and High-Throughput Screening in Drug Discovery*; CRC Press: Boca Raton, FL, USA, 2009.
33. Raimundo, L.; Espadinha, M.; Soares, J.; Loureiro, J.B.; Alves, M.G.; Santos, M.M.M.; Saraiva, L. Improving Anticancer Activity towards Colon Cancer Cells with a New P53-Activating Agent. *Br. J. Pharmacol.* **2018**, *175*, 3947–3962. [[CrossRef](#)]
34. Chou, T.-C.; Talalay, P. Quantitative Analysis of Dose-Effect Relationships: The Combined Effects of Multiple Drugs or Enzyme Inhibitors. *Adv. Enzym. Regul.* **1984**, *22*, 27–55. [[CrossRef](#)]